Applied Physics Letters

Terahertz detector based on a superconducting tunnel junction coupled to a thin superconductor film

Seiichiro Ariyoshi, Tohru Taino, Adrian Dobroiu, Hiromi Sato, Hiroshi Matsuo et al.

Citation: Appl. Phys. Lett. **95**, 193504 (2009); doi: 10.1063/1.3263711
View online: http://dx.doi.org/10.1063/1.3263711
View Table of Contents: http://apl.aip.org/resource/1/APPLAB/v95/i19
Published by the American Institute of Physics.

Terahertz detector based on a superconducting tunnel junction coupled to a thin superconductor film

Seiichiro Ariyoshi,[1,a)] Tohru Taino,[2] Adrian Dobroiu,[1] Hiromi Sato,[3] Hiroshi Matsuo,[4] and Chiko Otani[1,5]
[1]*Terahertz-wave Research Group, RIKEN, 519-1399 Aramaki-Aoba, Aoba-ku, Sendai 980-0845, Japan*
[2]*Saitama University, 255 Shimo-Ohkubo, Saitama 338-8570, Japan*
[3]*Radiation Laboratory, RIKEN, 2-1 Hirosawa, Wako, Saitama 351-0198, Japan*
[4]*National Astronomical Observatory of Japan, 2-21-1 Osawa, Mitaka, Tokyo 181-8588, Japan*
[5]*Tohoku University, 6-3 Aramaki-Aoba, Aoba-ku, Sendai 980-8578, Japan*

(Received 12 August 2009; accepted 22 October 2009; published online 13 November 2009)

The principle of a terahertz detector using a superconducting tunnel junction (STJ) coupled to a large terahertz-absorbing superconductor film is verified. We have detected terahertz radiation based on the Cooper-pair breaking process, and confirmed that the sensitivity has a sharp increase around 0.7 THz, a value that is in agreement with the gap frequency of the superconducting Nb. For high-sensitivity terahertz detection, we propose an improved design of the STJ detector composed of a smaller junction coupled to a thinner superconductor film. We also discuss the expected noise equivalent power of the optimized detector. © *2009 American Institute of Physics*.
[doi:10.1063/1.3263711]

New detector technologies in terahertz waves, or submillimeter waves, have enabled great advances in our understanding of the universe. The terahertz wave range is one of the essential bands for astronomical observations to survey primordial galaxies, which unveil galaxy formation and evolution in the early universe.[1] Terahertz waves are also used as a new diagnostic probe in various application fields such as industry, medicine, biology, and agriculture.[2] However, terahertz imaging devices with high sensitivity, broadband detection, and large array capability are still under development.

Semiconductor or superconductor bolometers are well developed as high-sensitivity cryogenic detectors of terahertz waves. However, bolometers are sensitive to operating temperature fluctuation, mechanical vibration, and electrical interference. Superconducting tunnel junction (STJ) detectors provide an excellent alternative. There are two kinds of direct detection mechanisms: the Cooper-pair breaking (CPB) and the photon-assisted tunneling (PAT).[3] The process choice is decided by whether the radiation frequency is greater or smaller than the superconductor gap frequency (ν_g). This ν_g is related to the critical temperature (T_c) of the superconductor material by $h\nu_g \simeq 3.52k_BT_c$: low T_c materials give effective terahertz detection, for example, around 0.7 THz for Nb (T_c=9.2 K) and 0.3 THz for Ta (4.4 K).

In previous reports, we have presented the development of two types of STJ direct detectors for the terahertz range. One type is based on the PAT process.[4] The other type, based on the CPB process, detects phonons generated in a terahertz-absorbing substrate.[5] Table I summarizes the performance comparison. The PAT-STJ detector has achieved a good noise-equivalent power (NEP): 1.6×10^{-16} W/$\sqrt{\text{Hz}}$.[6] However, its bandwidth is narrower than that of other STJ detectors and its array fabrication yield becomes lower since 12 linearly distributed STJs are needed for one detector pixel. On the other hand, the phonon-mediated STJ detector has advantages in terms of bandwidth and array fabrication, whereas the cold substrate acts as a low-absorption dielectric and propagation losses of phonons are inevitable. The resulting sensitivity becomes lower than for other STJ detectors. Another device, an antenna-coupled STJ detector, was proposed and tested at the Yale University.[7,8] In this detector, the ν_g of the metal film connecting to the superconductor antenna enforces confinement of the excitations in the STJ electrode. This detector has good potential for achieving a very high sensitivity within the limited bandwidth.

The STJ detector coupled to a thin superconductor film on a substrate, based on the CPB process, is a promising candidate in order to cover all of the advantages. In this type, the substrate provides the impedance matching with free-space radiation onto the thin film. The absorption efficiency of a superconductor film was theoretically analyzed in 1970,[9] and the basic idea of the detector was proposed in 1996.[10] In this paper, we describe its fabrication, and make a principle verification by measuring its spectral response in the terahertz region. Finally, we propose an improved design for a high detector performance.

As a first step in the principle verification of the STJ detector, we fabricated a prototype detector with a polycrystalline Nb absorber and a Nb-based STJ device, as shown in Fig. 1. The STJ devices were fabricated using a conventional

TABLE I. Comparison of terahertz-wave STJ detectors.

Detection Principle	NEP [W/$\sqrt{\text{Hz}}$]	High-sensitivity bandwidth and frequency	Array fabrication yield
PAT-STJ	$\sim10^{-16}$ (achieved)	$\sim$0.1 THz $\leq\nu_{g_{stj}}$	Low (12 STJs/pixel)
Phonon-mediated CPB-STJ	$\sim10^{-14}$ (achieved)	$\sim$10 THz $\geq\nu_{g_{stj}}$	High (1 STJ/pixel)
Antenna-coupled CPB-STJ	$\sim10^{-18}$ (expected)	$\sim$1 THz $\nu_{g_{ant}}\geq\nu\geq\nu_{g_{stj}}$	High (1 STJ/pixel)
Absorption film CPB-STJ	$10^{-17}\sim^{-18}$ (expected)	$\sim$10 THz $\geq\nu_{g_{film}}$	High (1 STJ/pixel)

a)Electronic mail: ariyoshi@riken.jp.

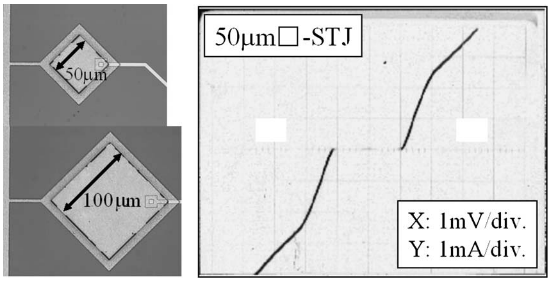

FIG. 1. Left: Microscope photographs of two detectors with different junction sizes (50 and 100 μm). They have the layer structure Nb/Al $-AlO_X$/Al/Nb=200/60/~1/60/150 nm on the sapphire substrate. Right: Typical *I-V* curve of the 50 μm-square junction at 1.5 K. The normal state resistance was 0.9 Ω, and the resulting critical current density was about 50 A/cm^2.

sputtering process, reactive ion etching and photolithography, as well as plasma oxidation for junction edges.[11] They have the layer structure Nb/Al$-AlO_X$/Al/Nb=200/60/ ~1/60/150 nm. The detector chip was attached to the backside of a silicon hyperhemispherical lens in a cryostat, and cooled to 0.3 K using liquid ^{4}He and a closed cycle ^{3}He sorption fridge. In order to suppress the dc Josephson current, a magnetic field of about 10 mT was applied using a NbTi superconducting Helmholtz coil.

To verify the performance of the absorption-film STJ detector, we have measured its spectral response. Figure 2 shows the spectrum taken by a Fourier-transform infrared spectrometer using a Martin–Puplett interferometer, in which a mercury-vapor lamp was employed as a broadband radiation source including the terahertz band. Sharp increase in sensitivity was observed around 0.7 THz at two different sizes of the detectors, where the 0.7 THz is in agreement with the ν_g of the superconducting Nb. We think the sensitivity peak just above the ν_g is mainly due to an enhancement in the superconducting absorptivity.[9] We have also observed a sensitivity peak at 0.5 THz in the larger size detector (100 μm square). We think this peak below the ν_g is a half-wavelength resonance depending on the absorber size (0.5 THz corresponds to a 200 μm wavelength in the sapphire substrate). Such a sensitivity peak is suppressed in the

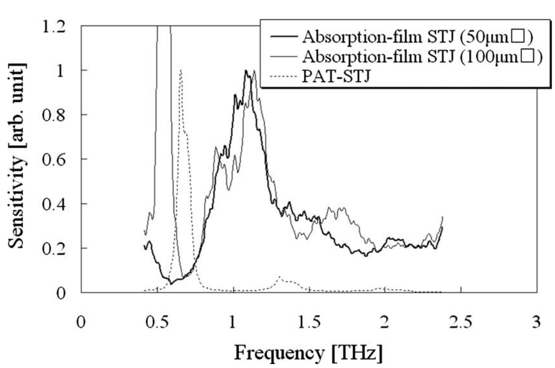

FIG. 2. Spectral response of the absorption-film STJ detectors (the two solid lines). The resolution of the spectrometer is 15 GHz. The broadband signals were observed from 0.7 up to 2.4 THz. The radiation above 2.4 THz was sharply cut by metal-mesh low-pass filters at the cryostat window. We have also excluded the data below 0.4 THz, where the source has a low spectral brightness. The spectrum of a PAT-STJ detector is superimposed for reference (dotted line) (Ref. 12). These three lines are normalized at their respective main peaks because of the different sensitivities of the detectors.

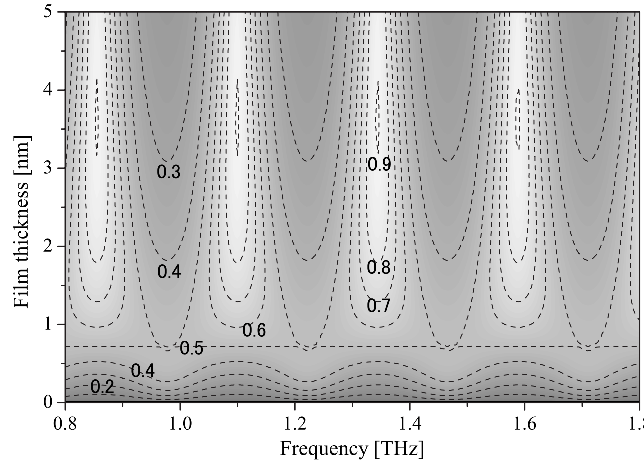

FIG. 3. Absorptivity of a normal-conducting Nb film as a function of frequency and film thickness. The contour step is 0.1 in absorptivity. This calculation was carried out using a sapphire substrate with n=3.07 and d =200 μm. A measured Nb-film resistivity at 4.2 K, $\rho_n=13.1\times10^{-8}$ Ω m (Ref. 14), was adopted for this calculation.

smaller size detector (50 μm square), and realizes pure high-pass characteristics at 0.7 THz.

The absorption-film STJ detector shows one order of magnitude broader spectral response at least, compared with the PAT-STJ detector having a 0.1 THz bandwidth (Fig. 2). This advantage will allow wide selectivity of observation frequency by employing various bandpass filters. However, the prototype detector has a low signal-to-noise ratio, which is probably because of the low absorption efficiency, estimated from the thick Nb film (200 nm) to be less than 3%.

In order to achieve a high absorption efficiency, we calculated the optimum film thickness on a sapphire substrate, which acts as an essentially lossless dielectric. The superconductor film asymptotically behaves as a normal conductor above ν_g.[9] The net absorptivity on the normal conductor film is given by Clarke *et al.*[13] as

$$A_n = \frac{T_1(1-T_2-R_2)}{1+R_1R_2 \pm 2\sqrt{R_1R_2}\cdot\cos\delta}, \quad (1)$$

where T_1 and R_1 are the transmission and reflection coefficients at the back surface of the substrate, T_2 and R_2 are those at the front surface, and δ corresponds to the phase of the radiation in the substrate. Figure 3 shows the absorption dependence of a normal-conducting Nb film as a function of frequency and film thickness. The absorptivity repeats in frequency with a period of cos δ, and its peaks and valleys strongly depend on the film thickness. The frequency-independent absorptivity of 0.5 requires a very thin film ($\simeq$1 nm), and a relatively high absorptivity requires a thickness of less than 10 nm.

Figure 4 shows a proposed design of the STJ detector. We need three additional solutions to achieve a high detector performance. The first is to utilize Al-based STJs, operated at 0.1 K, for the broader spectral response from millimeter waves. The second is to adopt a smaller junction to decrease the shot noise in the STJ leakage current. The third is to fabricate a highly uniform film to increase the collection efficiency of quasiparticles. A single-crystal Nb (or Ta) film is effective in reducing the losses through quasiparticle recombination because the electron lifetime in a single-crystal film is much longer than in a polycrystalline film.[15]

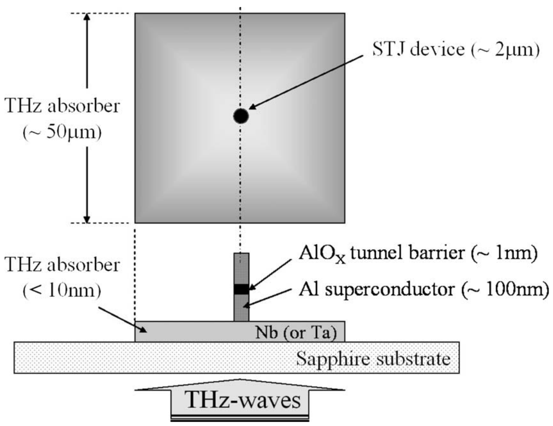

FIG. 4. Proposed design of the absorption-film STJ detector. The film thickness in this schematic is exaggerated for clarity.

The expected NEP of the detector under the low background condition is expressed by

$$\mathrm{NEP} = \frac{N}{\eta GS} = \frac{h\nu}{\eta GA} \cdot \sqrt{\frac{I_0}{2e}}[\mathrm{W}/\sqrt{\mathrm{Hz}}], \qquad (2)$$

where η is the coupling efficiency, G corresponds to the gain related to the back-tunneling effect,[16] S is the current responsivity ($=2eA/h\nu$), A is the number of broken Cooper pairs,[17] ν is the radiation frequency, I_0 is the leakage current, and N is the current noise ($=\sqrt{2eI_0}$). When I_0 is our achieved value of 6 pA, ν is 1 THz and η is 0.5, for example, the detector NEP could be as low as 6×10^{-18} W/$\sqrt{\mathrm{Hz}}$. This value is sufficient for a terahertz detector for ground-based astronomical observations and high-speed imaging applications.

We expect that future detector developments may come from the single-crystal fabrication of Al-based STJs as well as a terahertz-absorbing film. A polycrystalline STJ detector is currently dominated by the shot noise in the STJ leakage current that is much higher than the thermally excited leakage.[6] This fact implies that significantly lower NEP values can be achieved by reducing the leakage current. The probable origin of the excess leakage is thought to be due to the physical defects spread over the amorphous AlO_X barrier,[18] and/or the superconductor film quality.[19] Single-crystal fabrication would solve both problems. We think this attempt is worth trying, since single-crystal Fe/MgO/Fe magnetic tunnel junctions (MTJs) had a great success by forming a good wave function of electrons without scattering.[20] The MTJ has good similarity with the Al-based STJ in terms of crystal structure and lattice constant. The single-crystal fabrication may allow the STJ detector to become a fundamental technology toward future space missions that require high sensitivity.

The authors thank Professors Takashi Noguchi and Masahiko Kurakado for valuable discussions. This work was partly supported by the Grants-in-Aid under Grant No. 17686010, from the Ministry of Education, Culture, Sports, Science and Technology of the Japanese Government.

[1]A. W. Blain, I. Smail, R. J. Ivison, J.-P. Kneib, and D. T. Frayer, Phys. Rep. **369**, 111 (2002).
[2]Y.-S. Lee, *Principles of Terahertz Science and Technology* (Springer, New York, 2009).
[3]J. R. Tucker and M. F. Millea, Appl. Phys. Lett. **33**, 611 (1978).
[4]S. Ariyoshi, C. Otani, A. Dobroiu, H. Sato, K. Kawase, H. M. Shimizu, T. Taino, and H. Matsuo, Appl. Phys. Lett. **88**, 203503 (2006).
[5]T. Taino, R. Nakano, S. Yoshimura, H. Myoren, S. Takada, C. Otani, S. Ariyoshi, T. Shibuya, K. Kawase, H. Sato, and H. M. Shimizu, Nucl. Instrum. Methods Phys. Res. A **559**, 751 (2006).
[6]S. Ariyoshi, H. Matsuo, C. Otani, H. Sato, H. M. Shimizu, K. Kawase, and T. Noguchi, IEEE Trans. Appl. Supercond. **15**, 920 (2005).
[7]R. J. Schoelkopf, S. H. Moseley, C. M. Stahle, P. Wahlgren, and P. Delsing, IEEE Trans. Appl. Supercond. **9**, 2935 (1999).
[8]D. E. Prober, J. D. Teufel, L. Frunzio, C. M. Wilson, and R. J. Schoelkopf, Nucl. Instrum. Methods Phys. Res. A **559**, 676 (2006).
[9]M. Tinkham, in *Far Infrared Properties of Solids*, edited by S. S. Mitra and S. Nudelman (Plenum, New York, 1970), p. 223.
[10]H. Matsuo, T. Noguchi, A. Sakamoto, T. Sato, and S.-C. Shi, Proceedings of the 30th ESLAB Symposium, 1996 (unpublished), p. 37.
[11]H. Sato, Y. Takizawa, W. Ootani, T. Ikeda, T. Oku, C. Otani, H. Watanabe, K. Kawai, H. Miyasaka, H. Kato, H. M. Shimizu, H. Nakagawa, H. Akoh, M. Aoyagi, and T. Taino, Jpn. J. Appl. Phys., Part 1 **39**, 5090 (2000).
[12]S. Ariyoshi, C. Otani, A. Dobroiu, H. Matsuo, H. Sato, T. Taino, K. Kawase, and H. M. Shimizu, Jpn. J. Appl. Phys., Part 2 **45**, L1004 (2006).
[13]J. Clarke, G. I. Hoffer, P. L. Richards, and N.-H. Yeh, J. Appl. Phys. **48**, 4865 (1977).
[14]H. Matsuo, personal communication.
[15]G. Oya, M. Koishi, and Y. Sawada, J. Appl. Phys. **60**, 1440 (1986).
[16]D. J. Goldie, P. L. Brink, C. Patel, N. E. Booth, and G. L. Salmon, Appl. Phys. Lett. **64**, 3169 (1994).
[17]M. Kurakado, Nucl. Instrum. Methods Phys. Res. **196**, 275 (1982).
[18]K. Joosse, H. Nakagawa, H. Akoh, S. Takada, K. Maehata, and K. Ishibashi, Jpn. J. Appl. Phys., Part 1 **35**, 2633 (1996).
[19]T. Noguchi, T. Suzuki, A. Endo, and T. Tamura, Physica C **469**, 1585 (2009).
[20]S. Yuasa, T. Nagahama, A. Fukushima, K. Ando, and Y. Suzuki, Nature Mater. **3**, 868 (2004).